Available online at www.sciencedirect.com
SCIENCE DIRECT
Polymer 46 (2005) 2739–2747
polymer
www.elsevier.com/locate/polymer

Can rheometry measure crystallization kinetics? A comparative study using block copolymers

Antonis Kelarakis[a], Shao-Min Mai[a], Colin Booth[b], Anthony J. Ryan[a,*]

[a]*The Polymer Centre and Department of Chemistry, University of Sheffield, Sheffield S3 7HF, UK*
[b]*School of Chemistry, University of Manchester, Manchester M13 9PL, UK*

Received 5 November 2004; received in revised form 13 January 2005; accepted 18 January 2005

Abstract

The isothermal crystallization kinetics and the melting behavior of block copolymers of poly(ethylene oxide) and poly(1,2-butylene oxide) were studied by means of differential scanning calorimetry and rheometry to test the validity of rheological methods. The copolymers had different block lengths (hence different melt structures) and different block architectures (diblock EB and triblock EBE and BEB). For crystallization from disordered and lamellar melts, half-times for crystallization from rheometry were much shorter, and Avrami exponents were higher, than those from calorimetry. For more-highly structured melts (gyroid, hexagonal and cubic spheres), the half-times were comparable but the Avrami exponents from rheometry were still high compared to DSC. The differences between the rates of crystallization from calorimetry and rheometry are an artifact of the rheological measurements, at low crystallite volume fractions the rheology is directly proportional to the degree of crystallinity but at high crystalline volume fractions the proportionality is lost due to the changing connectivity of the crystals. The rates of crystallization ranked in order: lamellar > disordered ≈ gyroid > hexagonal ≫ cubic spheres. Other things being equal, the effect of block architecture was insignificant.

Keywords: Block copolymer; Crystallization; Rheometry

1. Introduction

Polymers crystallization has seen a great surge in interest recently [1] and a wide range of methods have been used to measure crystallization kinetics [2]. One method that is sometimes used is rheometry [3] and a critical test of this technique, for the study of crystallization in block copolymers, is reported here. The change in mechanical properties during crystallization is a complex function of the mass fraction of crystals and a mechanical model of the crystallizing polymer must be introduced. It is interesting to note that in one of the most careful rheometry studies [3] of crystallization the authors concluded that relating the rheological data to the degree of crystallinity was fraught with difficulty and that 'a single morphological model of the composite material cannot account for the evolution of the viscoelastic properties over the entire crystallization process.' This is borne out by the data reported here.

Block copolymers of type of E/B (E denotes an oxyethylene unit OCH_2CH_2 and B an oxybutylene unit $OCH_2CH(C_2H_5)$) exhibit a rich structural behavior because they combine one crystallizable E block and one non-crystallizable B block, this last reflecting the atactic configuration of the B block. Depending on block architecture, we denote these copolymers E_mB_n, $E_mB_nE_m$ and $B_nE_mB_n$, where m and n are the number-average block lengths in E and B repeat units. Microphase-separated structures may form from the melt when the temperature is lowered, by microphase separation in the melt state [4] and by crystallization of the E-block [5–9]. The melt-state phase diagrams for these copolymer have been determined (plotted as χr_v versus ϕ_E, where $\chi =$ the Flory–Huggins interaction parameter, $r_v =$ the chain length of the copolymer in segments of specified volume, $\phi_E =$ the volume fractions of the E blocks in the melt) and compared, one with another and with theory [4]. Moving across the phase diagram from low to high ϕ_E, the phases which have been

* Corresponding author. Tel.: +44 114 222 9409; fax: +44 114 222 9389.
E-mail address: tony.ryan@shef.ac.uk (A.J. Ryan).

0032-3861/$ - see front matter © 2005 Elsevier Ltd. All rights reserved.
doi:10.1016/j.polymer.2005.01.068

detected are body-centered cubic packed spheres (bcc), hexagonally packed cylinders (hex), a bicontinuous cubic structure with $Ia\bar{3}d$ symmetry (gyr), lamellae, gyr and hex.[4]

Crystallization during cooling at 10 °C min^{-1} has been investigated for diblock (EB) and triblock (EBE and BEB) copolymers [10–12]. The techniques used were differential scanning calorimetry (DSC) and synchrotron small-angle X-ray scattering (SAXS). Blending with poly(oxybutylene) (B) was used to control morphology in melts of EB copolymers which were otherwise lamellar [10,11]. The SAXS results showed that crystallization of cubic and hexagonal EB/B blends could either be confined to existing domains or could break out such that randomly branched fibrils of stacked lamellar crystals formed from many domains [10,11]. Confined crystallization was found when the crystallization temperature (T_c) was depressed by blending to a high volume fraction of B. As the Flory–Huggins interaction parameter for E and B segments (χ) increases with decrease in temperature, this meant that confined crystallization occurred when $\chi_c/\chi_{ODT} > 3$, where the subscripts denote χ at the crystallization temperature and the order–disorder temperature.[11] Crystallization of lamellar melts was unconfined. A wide range of unblended copolymers (EB, EBE and BEB) were investigated in subsequent work, but none met the conditions necessary for confined crystallization [12]. In related work it was shown that the orientation of lamellar crystals could be determined by pre-shearing a gyroid melt, but even so the crystallization was not confined [13].

Rates of isothermal crystallization of E/B copolymers and blends have been analysed [11,12] using the Avrami equation [14]

$$1 - X(t) = \exp(-kt^n) \quad (1)$$

where $X(t)$ is the fractional crystallinity at time t, k is the rate constant, and exponent n has characteristic values which reflect the dimensionality of growth and the nature of the nucleation and growth process. In confined crystallization from an ordered melt, when the morphology of the block copolymer is retained during crystallization, each separate domain crystallizes to completion after nucleation. Because of the much larger number of domains than heterogeneous nuclei in the system, crystallization is effectively initiated by homogeneous nucleation and, being sporadic in time, is a first-order process, i.e. the Avrami exponent $n = 1$. In contrast, break-out crystallization from an ordered melt (or crystallization from a disordered melt) leads to higher Avrami exponents. It was shown that isothermal crystallization of hexagonal and cubic melts of EB/B blends at low T_c did indeed conform to $n \approx 1$ [11]. At higher crystallization temperatures ($T_c = 30$–40 °C) values of $n \approx 3$ were found, consistent with break-out crystallization [11]. Similar values of $n \approx 3$ were found when hexagonal and cubic melts of non-blended block copolymers of all three architectures (EB, EBE and BEB) were crystallized isothermally at low temperatures, i.e. at undercoolings ($\Delta T = T_m - T_c$, where T_m is the melting temperature of the copolymer) of 50–70 °C [12]. Recently, Taden and Landfester have reported $\Delta T \approx 80$ °C for poly(oxyethylene) confined as droplets in an inverse mini-emulsion and cooled at 5 °C min^{-1} [15].

Here we report an extension of our investigation of the crystallization of E/B block copolymers, with the emphasis on the use of rheometry to study the kinetics of the process. The use of rheometry is based on the difference in elastic modulus between semi-crystalline and melt states. Floudas and coworkers have used the method with triblock copolymers of poly(ethylene oxide) and poly(styrene), type $E_mS_nE_n$ [S denotes $CH_2CH(C_6H_5)$], to identify melting temperatures and have explored its possible use in studying the rate of crystallization [16,17]. So far as the analysis of data for copolymers with disordered melts via the Avrami equation is concerned they showed, using samples of poly(ethylene oxide), that simple models [16,17] relating modulus to fractional crystallinity (X) were not adequate because of the percolation-induced change in modulus as the system changed from spherulites in an amorphous matrix at low crystallinity to amorphous domains in a semi-crystalline matrix at high crystallinity [17]. Use of the Rouse model [16] (parallel melt and solid phases) to obtain values of $X(t)$ from rheology data for poly(ethylene oxide) led to impossibly high values of the Avrami exponent, $n = 6$ or more, whereas $n = 2$, was obtained using data from DSC. For copolymer $E_{740}S_{650}E_{650}$ (our notation), where crystallization started from the microphase-separated lamellar state, the same value, $n = 2$, was obtained using both techniques [16].

We have studied the crystallization of twenty-one block copolymers with various block lengths and architectures (EB, BEB and EBE). The copolymers studied by Floudas and coworkers [16,17] contained long S blocks and the crystallization of the E-blocks was constrained by microphase separation of glassy poly(styrene) domains in the undercooled melt, particularly so at low crystallization temperatures, a condition characterized as hard confinement [18]. The B-block phase in microphase-separated melts of the present E/B copolymers is rubbery at normal temperatures, so-called soft confinement [18]. At the low values of the undercooling used in our work, $\Delta T = 4$–33 °C, confined crystallization was not expected. Our interest was in the possibility that rheometry might prove a satisfactory probe of the extent of crystallinity from ordered melts. Hamley et al. used rheology to follow the crystallization of a diblock copolymer of poly(ethylene oxide) and poly(isoprene), $E_{100}I_{79}$ (our notation, $I = CH_2CH{:}C(CH_3)CH_2$) from a pre-sheared hexagonal melt [19]. As in our work, the rubbery I-block phase provided soft confinement for crystallization of the E blocks, but rheology was not a major concern of that study.

2. Experimental section

2.1. Preparation and characterization of copolymers

The methods used in the synthesis of the copolymers by sequential anionic polymerization have been described previously [see the references in 4]. Gel permeation chromatography (GPC) was used to confirm narrow chain length distribution; for all the copolymers used in this work the ratios of number-to-mass-average molar mass M_w/M_n were found to be lower than 1.05. ^{13}C NMR spectroscopy was used to obtain absolute values of number-average molar mass, hence the average molecular formula and to confirm the architecture and sample purity. Formulas (see Table 1) are quoted as E_mB_n, etc. where m and n are known to 1%. Other quantities defined by previous work and relevant to the present studies are also listed in Table 1: the chain length of a copolymer in segments (r_v, segment volume the same as that of an E unit) and in nm (l), the volume fraction of the E blocks in the melt (ϕ_E), both calculated as described previously, [4] the temperature of the order–disorder transition (T_{ODT}), [4] the melting point of a slowly-cooled sample measured by DSC (T_m), [20] and the corresponding value of the parameter $f=(l/d)-1$ where l (in nm) is the chain length of a diblock copolymer or the half-chain length of a triblock copolymer, and d is the lamellar spacing measured by small-angle xray scattering [20]. Parameter f gives an indication of the extent of chain folding in the E blocks. Values are not expected to be integral, as discussed elsewhere [6–9].

2.2. Differential scanning calorimetry

A Perkin–Elmer Pyris-1 calorimeter was used. Samples of the copolymers (about 5 mg) were sealed into aluminum pans, heated to 75 °C, held for 5 min, then cooled at a rate of 10 °C min^{-1} to the crystallization temperatures and held at that temperature until crystallization was complete. The change of heat flow with time was recorded during crystallization.

The values of T_m reported in Table 1 refer to a slowly-cooled sample taken from storage in the freezer. Previous studies [5,6] have shown that this is a very good approximation to the equilibrium melting point for these polymers.

2.3. Rheology

A Rheometric Scientific dynamic stress rheometer (DSR-5000) with parallel plate geometry was used to measure storage and loss moduli. A stress-controlled instrument was chosen in order to accommodate the low modulus of the initial melt and the high modulus after crystallization in a single experiment. In the isothermal time scans, the samples were heated to an initial temperature of 75 °C and then cooled to different crystallization temperatures at a cooling

Table 1
Properties of the molten and semicrystalline copolymers

Copolymer	r_v	l (nm)	ϕ_E (melt)	T_{ODT} (°C)	T_m (°C)	$f=(l/d)-1$
Disordered melt						
$E_{134}B_{19}$	170	451	0.789	–	59.1	–
Lamellar melt						
$E_{60}B_{29}$	115	276	0.523	60	50.5	0.54
$E_{76}B_{38}$	148	354	0.514	114	52.1	0.89
$E_{85}B_{45}$	170	406	0.500	140	52.5	1.03
$E_{110}B_{30}$	167	422	0.660	85	57.4	1.40
$E_{114}B_{56}$	220	528	0.519	210	56.0	1.40
$E_{131}B_{35}$	197	500	0.664	133	58.0	1.56
$E_{155}B_{76}$	299	718	0.519	270	56.4	1.25
$E_{72}B_{68}E_{72}$	273	657	0.528	140	48.2	0.60
$E_{91}B_{56}E_{91}$	288	722	0.632	139	52.0	–
$E_{94}B_{46}E_{94}$	275	703	0.684	88	53.5	1.07
$B_{28}E_{182}B_{28}$	288	722	0.632	83	52.4	1.60
Gyroid melt						
$E_{75}B_{54}$	177	410	0.423	126	50.7	0.91
$E_{71}B_{79}E_{71}$	291	691	0.487	153	49.0	1.55
Hexagonal melt						
$E_{47}B_{62}$	164	359	0.286	93	42.8	0.66
$E_{64}B_{60}$	177	400	0.361	126	46.6	1.72
$E_{53}B_{86}E_{53}$	269	614	0.395	141	45.4	0.84
$E_{48}B_{100}E_{48}$	285	637	0.377	153	45.0	1.30
$E_{35}B_{114}E_{35}$	285	613	0.245	125	41.0	1.20
$B_{46}E_{99}B_{46}$	273	616	0.363	120	43.7	1.18
bcc melt						
$B_{49}E_{63}B_{49}$	248	535	0.254	55	37.4	1.08

Data from Refs. 4 and 20.

rate of 10 °C min^{-1}. Unless described otherwise, once the crystallization temperature had been reached the samples were immediately subjected to shear at frequency $\omega = 1$ rad s^{-1}, stress $\sigma = 250$ Pa (referred to as standard conditions in Section 3) and the modulus was recorded at ca. 20 s intervals.

2.4. Analysis of data

For isothermal DSC experiments, values of the mass fraction crystallinity at time t relative to $t = \infty$, $X(t)$, were calculated from:

$$X(t) = (\Delta_c H_\infty - \Delta_c H_t)/(\Delta_c H_\infty - \Delta_c H_o) \quad (2)$$

where $\Delta_c H_o$, $\Delta_c H_\infty$ and $\Delta_c H_t$ are enthalpies of crystallization before and after crystallization and at time t. The Avrami equation [14] was used in the form

$$\log[-\ln(1 - X(t))] = \log k + n \log(t) \quad (3)$$

to determine the rate constant k and exponent n. For isothermal rheology experiments, the parallel (Rouse) model was adopted and values of $X(t)$ (real or apparent depending on the system) were calculated from:

$$X(t) = (G_t - G_o)/(G_\infty - G_o) \quad (4)$$

where G_o, G_∞ and G_t are moduli before and after crystallization and at time t. Strictly speaking $X(t)$ calculated in this way is a volume fraction, assuming that the crystalline volumes are not continuous.

3. Results

3.1. Crystallization from disordered melts

Three commercial polyethylene glycols PEG4000 (E_{91}), PEG10000 (E_{227}) and PEG20000 (E_{455})] and one diblock copolymer with a disordered melt ($E_{134}B_{19}$) were used for investigation of the rheological method. Their chain lengths spanned the range of chain lengths of the copolymers. The results for all were essentially the same as those reported by Floudas and coworkers [16,17]. Those for $E_{134}B_{19}$ are summarized briefly below.

A typical curve of fractional crystallinity, $X(t)$, against time is shown in Fig. 1. The conditions for rheology (frequency $\omega = 1$ rad s^{-1}, external stress $\sigma = 250$ Pa) were those of choice for the copolymers with highly-structured melts and, as described in this and Section 3.2, were not optimized for disordered and lamellar melts. They are referred to as standard conditions. For copolymer $E_{134}B_{19}$ the nominal stress was not achieved in the early stages of the experiment where values of the strain amplitude (A) were very high, e.g. A approaching 10,000%. A was reduced as crystallization proceeded, to reach values approaching 0.002% as crystallization neared completion. Reducing the external stress to $\sigma = 100$ Pa increased the initial strain amplitude but, at the same time, increased the time for onset of crystallization. Increasing the frequency increased the onset time for crystallization and decreased the slope of $X(t)$, both effects leading to an increase in the time at which $X(t) = 1/2$, i.e. the crystallisation half-time $t_{1/2}$.

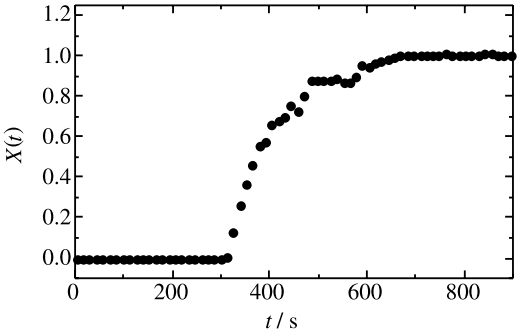

Fig. 1. Fractional crystallinity versus time determined by rheometry for the crystallization of copolymer $E_{134}B_{19}$ from its disordered melt. Conditions: $\omega = 1$ rad s^{-1}, $\sigma = 250$ Pa, $T = 53$ °C.

Half-times from DSC and rheometry are compared in Fig. 2. The overall result of using rheometry to probe crystallization from the disordered melt of copolymer $E_{134}B_{19}$ was to decrease $t_{1/2}$ by a factor of ten or more when compared with crystallization under quiescent conditions in DSC. No doubt this was a result of the large oscillatory strains experienced by the melts in the early stages of their crystallization. Orientation of the chains in a melt under high strain will reduce the entropy of crystallization without affecting the enthalpy of crystallization, thus increasing the effective melting point of the copolymer ($T_m = \Delta_{fus}H/\Delta_{fus}S = \Delta_{cryst}H/\Delta_{cryst}S$), and thereby increase the effective undercooling, and so the rates of crystal nucleation and growth [21,22].

Avrami analysis of the data obtained from DSC gave exponents in the range $n = 2$–3 whereas, as expected, [16] analysis of those obtained from rheometry ($\omega = 1$ rad s^{-1}, $\sigma = 250$ Pa) gave higher values, $n = 5$–6.

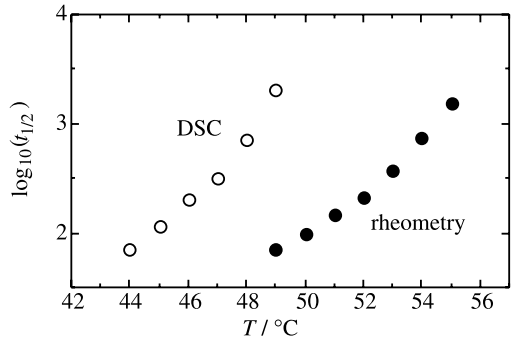

Fig. 2. Half-times determined by DSC and rheometry (as indicated) for the crystallization of copolymer $E_{134}B_{19}$ from its disordered melt. Conditions for rheometry: $\omega = 1$ rad s^{-1}, $\sigma = 250$ Pa.

3.2. Copolymers with lamellar melts

Seven diblock copolymers, three EBE triblock copolymers and one BEB triblock copolymer with lamellar melts (see Table 1) were investigated by rheometry under standard conditions. Copolymers $E_{60}B_{29}$, $E_{76}B_{38}$, $E_{110}B_{30}$, $E_{94}B_{46}E_{94}$ and $B_{28}E_{182}B_{28}$ were also investigated by DSC. Previous work had shown that break-out crystallization was the rule for copolymers of this type, certainly so for crystallization at small values of undercooling [12]. This was confirmed by Avrami analysis of the DSC data which led to values of exponent $n=2$–3, (ΔT in the range 5–17 °C). Values of n obtained by analysis of the rheology data were in the range 4–5, less extreme than the values found from rheometry for the polymers and copolymers with disordered melts, but still significantly different from the value obtained from DSC.

The rheological behaviour during crystallization was similar for all of these copolymers, including the effects of external shear and frequency. As an example, we describe the rheology of copolymer $E_{110}B_{30}$ studied under standard conditions. Because the melt was structured, its storage modulus was higher than that of the disordered melt of copolymer $E_{134}B_{19}$ and, as a consequence, the external stress of 250 Pa was maintained throughout the crystallization of copolymer. The strain amplitude in the early stages of crystallization under standard conditions was smaller than that observed for the disordered melt of $E_{134}B_{19}$, but even so it exceeded 1000%. Consequently the effects noted for disordered melts were reproduced for the lamellar melts, but were less extreme. This is illustrated in Fig. 3, where the half-time measured by rheometry for crystallization from the lamellar melt of copolymer $E_{110}B_{30}$ is seen to be a little less than half that from DSC, compared with less than one-tenth for crystallization from the disordered melt copolymer $E_{134}B_{19}$.

3.3. Copolymers with hexagonal, gyroid and bcc melts

Six copolymers with their E-blocks in cylindrical domains, one copolymer with its E blocks in spherical domains and two copolymers with E and B blocks in the interpenetrating domains of a gyroid phase (see Table 1) were investigated by rheometry under standard conditions. Five of the copolymers of the copolymers, $E_{75}B_{54}$ (gyr), $E_{47}B_{62}$, $E_{53}B_{86}E_{53}$, $B_{46}E_{99}B_{46}$ (hex) and $B_{49}E_{63}B_{49}$ (bcc), were also investigated by DSC. As illustrated in Fig. 4 for copolymer $E_{74}B_{54}$, values of the extent of crystallinity from rheometry and DSC were similar, although the slope of the plot of $X(t)$ versus $\log(t)$ was larger when determined by rheometry. Fig. 4 (gyroid melt) can be compared with Fig. 3 (lamellar melt).

The fair agreement of values of $t_{1/2}$ determined by DSC and rheometry illustrated in Fig. 4 was the rule for all the gyroid, hexagonal and bcc melts. Examples are shown in Fig. 5. This agreement of results from the two methods can be attributed to the high storage moduli of the highly-structured melts of these copolymers, which restricts the initial strain amplitude in oscillatory shear to a small value, typically $A \approx 1\%$.

Break-out crystallization was confirmed by Avrami analysis of the DSC data, which led to values of exponent n in the range 2–3 for all three melt structures (ΔT in the range 5–35 °C). Analysis of the rheometry data gave values of n in the range 3–4, consistent with the steeper slope of $X(t)$ from rheometry seen for copolymer $E_{74}B_{54}$ in Fig. 4.

4. Discussion

4.1. Melt structure and the Avrami exponent

Table 2 summarizes results for the copolymers investigated under standard conditions of frequency ($\omega=1$ rad s^{-1}) and external stress ($\sigma=250$ Pa) Important properties which determine the course of the crystallization are included. The values of the dynamic storage modulus and the strain amplitude at the beginning of the crystallization indicate the response of the melt to the applied sinusoidal stress, and the corresponding modulus at the end of the process indicates the state of the semicrystalline solid produced.

The Avrami exponent calculated from the rheometric data provides a measure of the abruptness of the change in

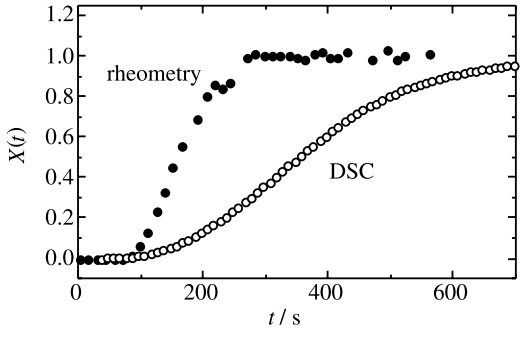

Fig. 3. Fractional crystallinity versus time determined by rheometry and DSC (as indicated) for the crystallization of copolymer $E_{110}B_{30}$ from its lamellar melt. Conditions: $\omega=1$ rad s^{-1}, $\sigma=250$ Pa, $T=46$ °C.

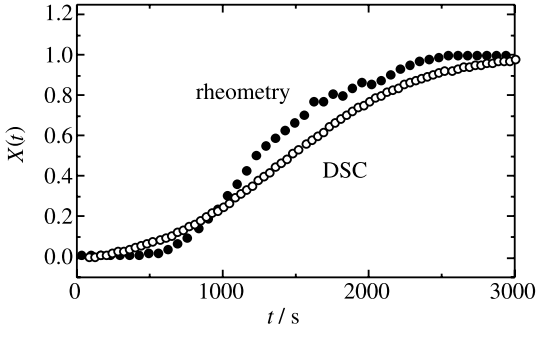

Fig. 4. Fractional crystallinity versus time determined by rheometry and DSC for the crystallization of copolymer $E_{74}B_{54}$ from its gyroid melt. Conditions: $\omega=1$ rad s^{-1}, $\sigma=250$ Pa, $T=42$ °C.

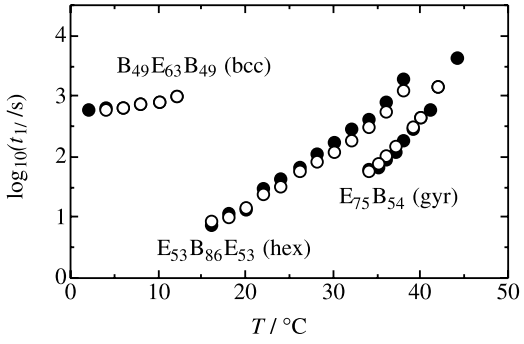

Fig. 5. Half-times determined by (○) DSC and (●) rheometry for the crystallization of copolymers from the gyroid, hexagonal and body-centred cubic melts indicated. Conditions for rheometry: $\omega = 1$ rad s^{-1}, $\sigma = 250$ Pa.

modulus during crystallization, and can be compared with Avrami exponents in the range 2–3 from DSC (not shown in Table 2) to gain an indication of the reliability of the rheometric method under the conditions investigated. The fact that the Avrami exponent from DSC falls into a narrow range of values ($n = 2$–3) for all the samples investigated indicates that the crystallization process follows a similar course albeit at different rates (see Section 4.2) irrespective of the structure of the melt. A value of $n = 3$ corresponds to a nucleation by heterogeneities and three-dimensional (spherulitic) growth, while somewhat lower values suggests a contribution from growth with lower dimensionality. Optical microscopy of EB copolymers [10] shows spherulites, when the Avrami exponent is ~3, implying linear linear growth of fibrils.

With respect to rheometry, an obvious feature of Table 2 is the very large strain amplitude caused by the low elastic moduli ($G' \leq 1$ kPa) of the disordered and lamellar melts. Presumably this leads to orientation of chains in the early stages of the process, and so to excess crystallization compared to quiescent conditions, [23] resulting in the observed high values of the Avrami exponent ($n \geq 4$). The higher elastic moduli of the gyroid, hexagonal and cubic melts ($G' = 10$–100 kPa) moderate this effect but do not remove it entirely, as shown by Avrami exponents in the range 3–4 compared with 2–3 from DSC. Crystallization from the hexagonal and cubic melts leads finally to solids with significantly lower elastic moduli, suggestive of a rubbery matrix reinforced by crystalline domains rather than a continuous polycrystalline phase. Even so, the Avrami analysis favours break-out crystallization with connected crystals.

4.2. Melt structure and the rate of crystallization

The polymers that crystallised from lamellar and disordered phases had anomalously high rates of crystallisation by rheometry. This is a result of the measurements which were made at a 'standard' stress. Due to the low viscosity in the melt they experience a large number of shear units prior to crystallisation—this causes the enhanced nucleation. The polymers that have hexagonal and cubic morphologies have a lower E content but a higher melt viscosity, consequently they do not experience high shear

Table 2
Crystallization of block copolymers

Copolymer	Melt	T_m (°C)	ΔT, °C (range)	Rheometry[a]			
				G', kPa (initial)	A, % (initial)	G', Mpa (final)	n
$E_{134}B_{19}$	dis	59.1	4–15[b]	[c]	5000	14	5–6
$E_{60}B_{29}$	lam	50.5	7–17	[c]	1500	10	4–5
$E_{76}B_{38}$	lam	52.1	4–14	0.02	1500	11	4–5
$E_{85}B_{45}$	lam	52.5	6–14	0.01	1000	11	4–5
$E_{110}B_{30}$	lam	57.4	7–14	0.02	1000	17	4–5
$E_{114}B_{56}$	lam	56.0	9–16	0.08	600	15	4–5
$E_{131}B_{35}$	lam	58.0	6–18	0.06	1000	14	4–5
$E_{155}B_{76}$	lam	56.4	6–14	0.12	600	7	4–5
$E_{72}B_{68}E_{72}$	lam	48.2	5–13	0.13	500	14	4–5
$E_{91}B_{56}E_{91}$	lam	52.0	5–12	0.22	300	11	4–5
$E_{94}B_{46}E_{94}$	lam	53.5	5–14	0.18	500	16	4–5
$B_{28}E_{182}B_{28}$	lam	52.4	5–12	1.3	7	9	4–5
$E_{75}B_{54}$	gyr	50.7	7–17	1200	0.2	10	3–4
$E_{71}B_{79}E_{71}$	gyr	49.0	7–16	1100	0.05	11	3–4
$E_{47}B_{62}$	hex	42.8	10–21	200	0.5	2	3–4
$E_{64}B_{60}$	hex	45.1	5–14	200	1	2	3–4
$E_{53}B_{86}E_{53}$	hex	45.4	7–29	300	0.2	3	3–4
$E_{48}B_{100}E_{48}$	hex	45.0	15–29	400	0.3	2	3–4
$E_{35}B_{114}E_{35}$	hex	41.0	27–34	800	0.3	2	3–4
$B_{46}E_{99}B_{46}$	hex	43.7	12–24	500	0.1	2	3–4
$B_{49}E_{63}B_{49}$	bcc	37.4	25–33	1000	0.2	1	3

[a] Standard conditions: $\omega = 1$ rad s^{-1}, $\sigma = 250$ Pa. Approximate median values of G' and A for the temperature range studied.
[b] $\Delta T = 4$–10 °C (rheometry) and 10–15 °C (DSC).
[c] G' too low to measure.

prior to crystallisation and there is no rheometric enhancement of the rate of crystallisation.

In order to compare the crystallization rates of the various copolymers it is necessary to account for differences in melting point and crystallization temperature. Assuming heterogeneous nucleation and break-out growth of lamellar crystals determined by single monolayer nucleation, and slow kinetics, the crystallization process should be in regime I [21,22]. The crystallisation rates are necessarily slow, in order to be able follow them by rheometry, so regime III at high undercoolings will not apply [21,22]. Even if the rates are not low enough for Regime I, the formal equations are the essentially the same for regimes I and II with just a difference in numerical factor. As we are not using the analysis to determine linear growth rates, we use the simpler form. The growth rate of a crystal (ν) can be written [21,22]

$$\nu = \nu_o \exp(-\Delta F_\eta/kT) \exp(-\Delta F^*/kT) \quad (5)$$

where ν_o is independent of temperature and the last two terms account for the Gibbs energies of transport across the melt/crystal interface and the requirement of a critical nucleus size. At small undercoolings and over a limited temperature range, the temperature dependence of growth is determined predominantly by the nucleation term. This term can be written

$$a\Delta F^* = C(T_m^e/\Delta T) \quad (6)$$

where T_m^e is the equilibrium melting temperature of the sample, $\Delta T = (T_m^e - T_c)$ is the undercooling and factor C, which depends directly on the Gibbs energies of formation of lateral and end faces of the lamellar crystal and inversely on the enthalpy of formation of crystal from melt, is effectively independent of temperature over a limited range [21,22]. Accordingly, assuming that the inverse half-time is a satisfactory measure of the rate of crystallization, we plot the data as $\log(1/t_{1/2})$ versus $T_m/(T_c\Delta T)$: see Fig. 6. It is assumed that the melting temperatures taken from Table 1 approximate the equilibrium values. For clarity not all data sets are included. Comparison of Fig. 6a (DSC) with Fig. 6b (rheometry) shows the accelerating effect of the large strain-amplitude, induced by oscillatory shear under the conditions of our experiments, for copolymers with lamellar melts (filled circles) and, particularly, for the copolymer with the disordered melt (unfilled circles). Because of this, the effect of melt structure is most clearly seen in Fig. 6a (DSC).

Within the scatter of the data points, and considering only crystallization from relatively unperturbed melts (i.e. from DSC and from rheometry for gyr, hex and bcc melts), the rates of crystallization at equivalent values of the undercooling parameter rank approximately as lam > dis ≈ gyr > hex ≫ bcc. This broad ranking is understandable: lamellar melt to lamellar crystal involves minimum reorganisation of E blocks, while a bcc melt (to a lesser extent a hexagonal melt) maximizes separation of E blocks prior to formation of lamellar crystals and involves higher interfacial energy barriers.

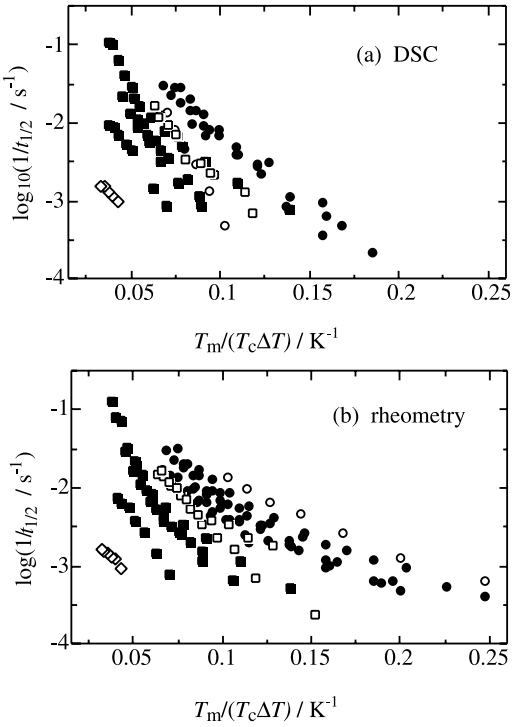

Fig. 6. Inverse half-times determined by (a) DSC and (b) rheometry for the crystallization of copolymers from the melt: (○) disordered, (●) lamellar, (□) gyroid, (■) hexagonal, (◇) bcc. Conditions for rheometry: ω = 1 rad s^{-1}, σ = 250 Pa.

4.3. Effect of block architecture

The overall impression from the plots in Fig. 6 is that the half-times of crystallization are not very dependent on block architecture. This is examined in more detail in Fig. 7, in which the half-times from DSC are plotted for three copolymers with lamellar melts and three copolymers with hexagonal melts. Within each set the copolymers have

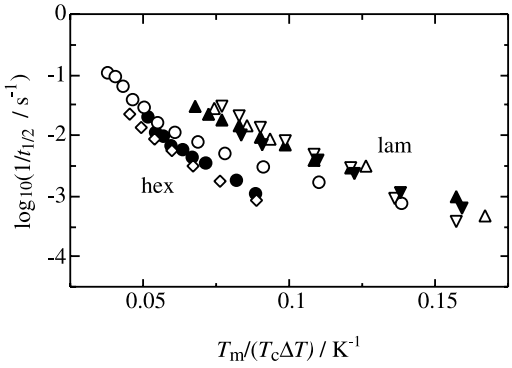

Fig. 7. Inverse half-times determined by DSC for the crystallization of copolymers from hexagonal and lamellar melts, as indicated: (●) $E_{47}B_{62}$, (○) $E_{53}B_{86}E_{53}$ and (◇) $B_{46}E_{99}B_{46}$ (all hexagonal); (△) $E_{76}B_{38}$, (▲) $E_{60}B_{29}$, (▽) $E_{94}B_{46}E_{94}$ and (▼) $B_{28}E_{182}B_{28}$ (all lamellar).

similar E-block lengths, counting half-length in the case of the BEB copolymers. Given that adjustment, there is no discernible effect of block architecture for the copolymers with lamellar melts, and essentially no effect for those with hexagonal melts. The deviation seen for copolymer $E_{53}B_{86}E_{53}$ at low values of the undercooling is discussed in Section 4.4.

4.4. Chain folding

If the nucleation term in Eq. (5) is dominant and the factor C in Eq. (6) is constant then, in Figs. 6 and 7, the data points for a given copolymer should fall onto a straight line. Inspection of the plots in Fig. 6 shows that this is not always the case. Fig. 8 shows data for copolymers $E_{53}B_{86}E_{53}$ and $E_{94}B_{46}E_{94}$. These results are chosen for illustration because they were obtained over relatively wide temperature ranges, $\Delta T = 7$–29 and 4–14 °C, respectively. For copolymer $E_{53}B_{86}E_{53}$ with a hexagonal melt the results from rheometry and DSC are similar. A change in slope at $T_m/(T_c\Delta T) \approx 0.06$ corresponding to $\Delta T \approx 16$ °C ($T_c \approx 29$ °C) is obvious. This discontinuity in slope is attributed to a change in chain folding. Similar changes in the dependence of crystallization rate on undercooling have been found for polyethylene glycols [24] and related dimethyl and diethyl ethers [25]. The slope is high for an interface with a high proportion of chain folds because the value of the Gibbs energy of formation of a folded-chain lamellar-crystal surface is high compared to one formed from chain ends [26]. Considering the folding parameter from SAXS listed for copolymer $E_{53}B_{86}E_{53}$ in Table 1 ($f \approx 1$, once-folded chain, unfolded E-blocks), the change is probably from once-folded E-blocks (at large ΔT) to unfolded E-blocks (at small ΔT). That the transition is from folded to unfolded blocks, rather than a regime transition, is supported by previously reported studies by SAXS [6,7,10–12] and Raman Spectroscopy [6,8,9].

As discussed in Section 3.2, for copolymer $E_{94}B_{46}E_{94}$ only data from DSC are reliable in an absolute sense. However, the change in slope in the data from rheology occurs at the same position on the abscissa scale as that defined by DSC, and may be regarded as supporting evidence. For this copolymer there is a change in slope at $T_m/T_c\Delta T \approx 0.15$ corresponding to $\Delta T \approx 7$ °C ($T_c \approx 47$ °C). Again the change is probably from once-folded E-blocks to unfolded E-blocks as ΔT is decreased. Related experiments in which d-spacings were measured[20b] for this copolymer crystallized at large ΔT (cooled, $f \approx 1$) and small ΔT (self-seeded, $f \approx 0$) confirmed the assignment.

5. Conclusions

Our investigation highlights a number of problems when using oscillatory rheometry to study the rate of crystallization of block copolymers. Because strain-controlled rheometry does not have the sensitivity to cover the range of dynamic modulus involved in going from a mobile melt to a semicrystalline solid, it is necessary to use stress-control. However, with stress control the mechanical response is highly dependent on the structure of the initial melt. The response of low-modulus disordered and lamellar melts is a large strain amplitude, which through orientation of the melt increases the rate of crystallization in its initial stages. Perturbation of the more structured, high modulus hexagonal, gyroid and cubic melts is unimportant, and half-times for crystallization are comparable with those obtained under quiescent conditions by DSC. However, in the later stages of crystallization the rheological response is dominated by percolation-induced structure formation, leading to a rapid change of modulus, and thereby anomalously high values of the Avrami exponent n even for well-structured melts.

If rheological investigations are restricted to determination of $\Delta T_{1/2}$, the method can be used to study the rate of crystallization of copolymers with hexagonal, gyroid or cubic melts. In this study, supplementing the rheological measurements where necessary by results obtained using DSC, we have shown that rates of crystallization determined for a wide range of copolymers are dominated by melt structure and rank in order: lam > dis ≈ gyr > hex ≫ bcc. The ranking lam > dis ≈ gyr reflects the ease of reorganization in forming lamellar crystals from these melts. The

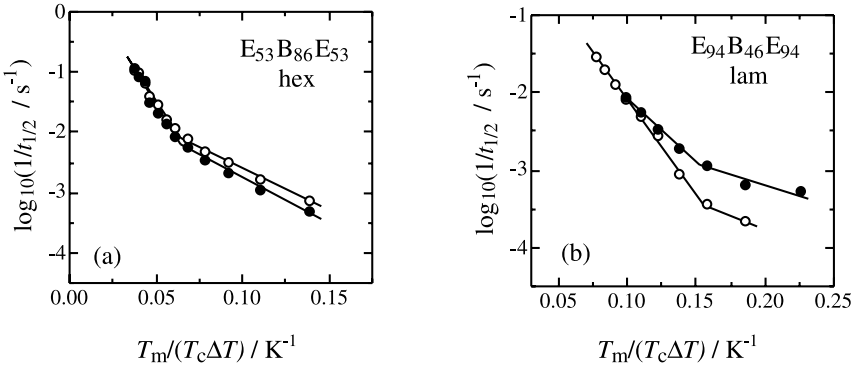

Fig. 8. Inverse half-times determined by (○) DSC and (●) rheometry for the crystallization of the block copolymers indicated. Conditions for rheology: $\omega = 1$ rad s^{-1}, $\sigma = 250$ Pa.

ranking gyr > hex ≫ bcc reflects the increasing importance of interfacial energy.

It is interesting that even for lamellar melts the temperature dependence of $\Delta T_{1/2}$ from rheology can provide a satisfactory indication of the temperature of onset of chain folding in isothermal crystallization.

Overall, however, when compared with conventional methods such at DSC, dilatometry and X-ray scattering, the disadvantages in using oscillatory rheology to study the crystallization of copolymers far outweigh any perceived advantages.

Acknowledgements

AK was supported by the EU-TMR network. Copolymer synthesis in Manchester was supported by EPSRC.

References

[1] See, for example (a) Strobl G. Eur Phys J 2000;E3:165.
(b) Lotz B. Eur Phys J 2000;E3:185.
(c) Cheng SZD, Li CY, Zhu L. Eur Phys J 2000;E3:195.
(d) Muthukumar M. Eur Phys J 2000;E3:199.
[2] Strobl G. The physics of polymers. Berlin: Springer; 1997.
[3] Leelinger C, Floudas G, Alig I. Polymer 2003;44:5759.
[4] Ryan AJ, Mai S-M, Fairclough JPA, Hamley IW, Booth C. Phys Chem Chem Phys 2001;3:2961.
[5] Ryan AJ, Fairclough JPA, Hamley IW, Mai S-M, Booth C. Macromolecules 1997;30:1727.
[6] Mai S-M, Fairclough JPA, Viras K, Gorry PA, Hamley IW, Ryan AJ, et al. Macromolecules 1997;30:8392.
[7] Chaibundit C, Mingvanish W, Booth C, Mai S-M, Turner SC, Fairclough JPA, et al. Macromolecules 2002;35:4838.
[8] Viras K, Kelarakis A, Havredaki V, Mai SM, Ryan AJ, Mistry D, et al. J Phys Chem B 2003;107:6946.
[9] Viras K, Mai SM, Ryan AJ, Yu G-E, Booth C, Chaibundit C. Macromolecules 2004;37:3077.
[10] Xu J-T, Turner SC, Fairclough JPA, Mai S-M, Ryan AJ, Chaibundit C, et al. Macromolecules 2002;35:3614.
[11] Xu J-T, Fairclough JPA, Mai S-M, Ryan AJ, Chaibundit C. Macromolecules 2002;35:6937.
[12] Xu J-T, Fairclough JPA, Mai S-M, Chaibundit C, Mingvanish W, Booth C, et al. J Polym 2003;44:6843.
[13] Fairclough JPA, Mai S-M, Matsen MW, Bras W, Messe L, Turner SC, et al. J Chem Phys 2001;114:5425.
[14] Avrami MJ. Chem Phys 1939;7:1103.
[15] Taden A, Landfester K. Macromolecules 2003;36:4037.
[16] Floudas G, Tsitsilianis C. Macromolecules 1997;30:4381.
[17] Alig I, Tadjbakhsch S, Floudas G, Tsitsilianis C. Macromolecules 1998;31:6917.
[18] See, for example, Zhu L, Mimnaugh BR, Ge Q, Quirk RP, Cheng SZD, Thomas EL, et al. Polymer 2001;42:9121.
[19] Hamley IW, Castelletto V, Floudas G, Schipper F. Macromolecules 2002;35:8839.
[20] (a) PhD Theses, University of Manchester: Mai S-M (1996), Chaibundit C (2001), Mingvanish W (2001). (b) Turner SM, PhD Thesis, University of Sheffield; 2000.
[21] Wunderlich B. Macromolecular physics. Crystal nucleation, growth, annealing. vol. 2. New York: Academic Press; 1976.
[22] Mandelkern L. Crystallization of polymers. New York: McGraw-Hill; 1964.
[23] See, for example, Kornfield JA, Kumaraswamy G, Issaian AM. Ind Eng Chem Res 2002;41:6383.
[24] (a) Kovacs AJ, Gonthier A. Kolloid Z Z Polym 1972;250:530.
(b) Kovacs AJ, Gonthier A, Straupe C. J Polym Sci, Polym Symp 1975;40:283.
[25] Fraser MJ, Marshall A, Booth C. Polymer 1977;18:93.
[26] See, for example, Yang Z, Cooke J, Viras K, Gorry PA, Ryan AJ, Booth C. J Chem Soc, Faraday Trans 1997;93:4033.